Silicon Carbide-Strengthened Magnetorheological Elastomer: Preparation and Mechanical Property

Jie Yang, Xinglong Gong, Luhang Zong, Chao Peng, Shouhu Xuan
Department of Modern Mechanics, CAS Key Laboratory of Mechanical Behavior and Design of Materials, University of Science and Technology of China, Hefei 230027, People's Republic of China

A novel silicon carbide (SiC)-strengthened magnetorheological elastomers (MREs) was developed to enhance its viscoelastic performance. The influences of the size and weight content of the SiC particles on the viscoelastic performance of the MREs were systematically studied. The shear storage modulus, damping property, and magnetorheological effects were analyzed to evaluate their dynamic properties. Under optimum condition, the initial storage modulus (G_0) of the MRE-0.06-SiC-3 (SiC weight content 3.2 wt%, mean diameter 0.06 μm) is about 2.16 times larger than the MRE-0.06-SiC-0 (nondoped MRE), whereas the magnetorheological effect was almost kept constant. In addition, the damping properties of the as-prepared MREs which were obtained from the intrinsic damping, the magneto-mechanical hysteresis, and the interface damping were also analyzed. These results provided a meaningful method for developing MREs with controllable storage modulus and damping capacity. POLYM. ENG. SCI., 53:2615–2623, 2013. © 2013 Society of Plastics Engineers

INTRODUCTION

Magnetorheological (MR) materials have attracted a wide variety of attention because of their controllable and reversible mechanical properties under applying the external magnetic field [1–4]. Magnetorheological elastomer (MRE), which was usually prepared by dispersing micron-sized soft magnetic particles into the nonmagnetic matrix, was an important branch of MR materials [5–7]. During the preparation, the magnetic particles were assembled to form chain-like or column-like structures in the curing process owing to the presence of the magnetic field, and thus the as-formed MREs exhibited an anisotropic property. As the magnetic particles were locked within the polymer matrix, the sedimentation, instability, and leakage problem can be avoided in the MREs. As a solid analogy of MR fluids, the MREs have been proven to be the critical components for their applications in damper [8], brake [9], vibration control [10], isolator [11], and so on [12–14].

Coupling the magnetic field and strain field together in the MREs has given rise to a series of interesting magneto-mechanical properties, which were the key factors that determine the application of MREs. To comprehensively investigate the dynamic mechanical properties of MREs, various efforts have been conducted to manufacture the high-performance MREs [15–18]. The mechanical and magnetic properties of the MREs were substantially affected by the matrix, size, and shape of the magnetic particles, arrangement of magnetic particles, and the additives. Demchuk et al. [19] systematically investigated the influence of different types of matrix, different sized ferromagnetic filling particles, and the intensity of external magnetic field on the MREs' performance. Lokander and Stenberg [20] observed that the MREs with larger iron particles exhibited larger magnetorheological effect. Recently, Li et al. [21] reported that prestructure process showed a significant influence on magnetorheological effect. To synthesize high-performance MREs, Li and Zhang [22] introduced second kind of magnetic particles into the traditional MREs and developed the bimodal magnetic particle-based MREs. In comparison to the monomodal MREs, an enhanced magnetorheological effect can be obtained. Very recently, by introducing the MRG and MRF component into the MRE matrix, Zhang et al. [23] exploited a novel kind of hybrid MREs, in which the MRG-based hybrid MREs exhibited higher mechanical properties than the MRF-based one.

To date, the introduction of the additives into the MR materials could also significantly improve their magneto-induced properties. By using the Fe nanowires as the additives, Jiang et al. [24] developed a dimorphic MRF in which the yield stress of the MRF was highly enhanced. Owing to the entanglement of the nanowires, the as-prepared dimorphic MRF also exhibited a better sedimentation property than the traditional one. Chen et al. [25] reported that the carbon black could be employed as an effective additive to improve the mechanical property of the MREs. The pres-

Correspondence to: Xinglong Gong; e-mail: gongxl@ustc.edu.cn
Contract grant sponsor: The National Natural Science Foundation of China; contract grant numbers: 11125210, 11072234, 11102202; contract grant sponsor: The National Basic Research Program of China (973 Program); contract grant number: 2012CB937500; contract grant sponsor: The Specialized Research Fund for the Doctoral Program of Higher Education of China (Project No.20093402110010).
DOI 10.1002/pen.23529
Published online in Wiley Online Library (wileyonlinelibrary.com).

ence of the carbon black was of benefit to generate a well-bond microstructure, so that the MR effect could be increased, the damping ratio was decreased, and the tensile strength was improved. During the past decades, various additives such as the FeSi, Fe_3O_4, γ-Fe_2O_3, $SrFe_{12}O_{19}$, $BaCo_xTi_xFe_{12-2x}O_{19}$, magnetic metallic glasses, maleic anhydride, thermoplastic polymer polycaprolactone, and intrinsically ferromagnetic pure polymers have been introduced into the MRE matrix [26–29], and the mechanical properties were enhanced relatively. However, the detailed mechanism for the improvement of the dynamic property has not been systematically investigated. Various problems such as the influence of the content and the size of the additive on the mechanical behavior of the MREs still existed.

In this study, a novel kind of silicon carbide (SiC)-strengthened MREs was developed to improve the dynamic mechanical performance of MREs. The SiC particles have been widely used in rubber technology as they bond well with the rubber matrix, and they can significantly ameliorate the performance of rubber materials [30–32]. To investigate their structure-dependent properties, a series of SiC-strengthened MREs with different SiC weight fractions and sizes were synthesized. The performance of these SiC-strengthened MREs was improved under optimizing the manufacture process. To our knowledge, this was the first report on analyzing how the size, content, assembling structure of the additives affect the viscoelastic performance of the MREs. The mechanism for the SiC additive-dependent storage modulus and damping was carefully investigated. This study is not only helpful to understand the enhancing mechanism of the additives but also provides a feasible way to synthesize MREs with enhanced performances.

EXPERIMENTAL

Preparation of SiC-Strengthened MREs

In this experiment, SiC-strengthened MREs with different contents and sizes of nonmagnetic SiC particles were prepared, respectively. The matrix material was natural rubber (NR) and the magnetic particles were carbonyl iron (CI) particles (the average diameter is 6 μm, brought from BASF). The SiC particles were of different diameters, 0.06, 0.6, 6, and 60 μm, and they were brought from Xuzhou Jiechuang New Material Technology, China. The fabrication progress of the SiC-strengthened MREs consisted of three steps: mixing, preconfiguration, and curing. During the fabrication, the CI particles, SiC particles, and other additives were mingled into the rubber matrix in a double-roll mill so that all components were mixed homogeneously. Then, the product was compressed into a mold for preforming under an external magnetic field of 1.3 T generated by a self-developed magnetic-thermocoupling device at 80°C for 15 min. After this procedure, the mixture was vulcanized at 153°C for 10 min under a pressure of 1.5 atm. Finally, the fabrications of the MRE samples were completed.

To optimize the SiC size, four MREs samples incorporating were fabricated different diametric SiC particles (0.06, 0.6, 6, and 60 μm). The SiC particles' weight content in these four groups of MREs was maintained 10%. The as-prepared SiC-strengthened MREs were defined as MRE-0.06-SiC, MRE-0.6-SiC, MRE-6-SiC, and MRE-60-SiC accordingly. In addition, a series of SiC-strengthened MREs with different weigh contents of 0.06 μm SiC were denoted as MRE-0.06-SiC-1, MRE-0.06-SiC-2, MRE-0.06-SiC-3, and MRE-0.06-SiC-4, in which the SiC particle contents were 0, 1.6, 3.2, and 4.8 wt%, respectively. For all the samples, the weight ratios of the CI particles to the NR matrix were kept at 150 wt%.

The Structure Characterization and the Mechanical Properties of the SiC-Strengthened MREs

The microstructures of the samples were characterized by environmental scanning electron microscopy (SEM, Philips of Holland, model XL30 ESEM-TMP) with an accelerating voltage of 20.0 kV. A rheometer (Physica MCR 301, Anton Paar) was used to measure the dynamic properties. The sample was placed between the rotating disk and the base, both of them were made of nonpermeable materials, and then a fixed oscillatory strain was applied on the rotating plate. Testing temperatures were controlled by a fluid circulator with water, and a magnetic field strength was adjusted by controlling the current in the electromagnetic coil. Each sample is 20 mm in diameter and 1 mm in thickness. The MRE samples were tested under different strain amplitudes (0.2, 0.4, 0.6, 0.8, and 1%) together with different magnetic fields (from 0 to 0.95 T), respectively. The shear frequency was 10 Hz. All tests were operated at a constant temperature of 25°C.

RESULTS AND DISCUSSIONS

The Influence of the SiC Particles on the Storage Modulus of the SiC-Strengthened MREs and Their Microstructure

Owing to their high compatibility, the SiC particles were proven to be an ideal additive to strengthen the polymer-based materials. After introducing the SiC particles into the traditional MREs, the dynamic mechanical properties of the MRE materials changed significantly. Figure 1 shows the magnetic-dependent shear storage modulus (G) of the as-prepared SiC-strengthened MREs. With increasing of the magnetic field, the storage modulus increases, indicating all the SiC-strengthened MREs exhibited a typical MR behavior. To optimize the strengthening effect, SiC particles with diameters from 0.06 to 0.6, 6, and 60 μm were employed to synthesize the SiC-strengthened MREs. In comparison to the traditional MREs, the SiC-strengthened MREs showed a strengthening nature. First, as soon as the SiC particles

 DOI 10.1002/pen

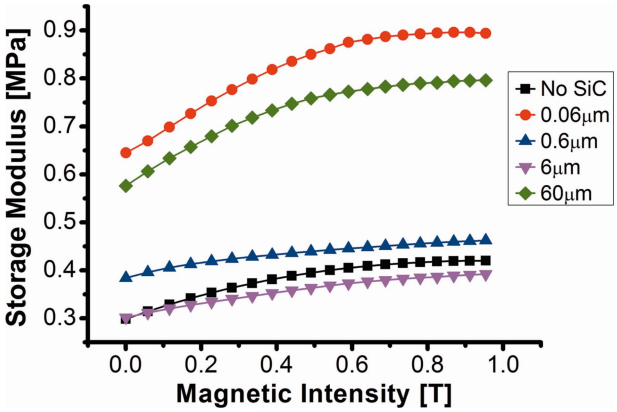

FIG. 1. The storage modulus of different diametric MRE samples. The samples are tested at the strain amplitude of 0.2%. [Color figure can be viewed in the online issue, which is available at wileyonlinelibrary.com.]

were introduced into the MREs, the initial shear modulus G_0 increased, indicating the product became harder. Interestingly, if the size of the SiC particles was larger or smaller than 6 μm (similar to the size of the CI particles), the G_0 increased, whereas the 6-μm SiC-strengthened MREs exhibited a similar G_0 value (0.3016 MPa) to the nonstrengthened MREs (0.2987 MPa). This result indicated that the G_0 depended on the size of the doping particles. Second, with increasing of the magnetic field, the magneto-induced modulus (ΔG) was highly influenced by the diameters of the SiC particles. For the 0.06-μm SiC-strengthened MREs, the ΔG was 0.25 MPa and this value was larger than the nonstrengthened MREs (0.12 MPa). With further increasing the size of the SiC particles from 0.6 to 6 and 60 μm, the ΔG irregularly increased to be 0.08, 0.09, and 0.22 MPa, respectively.

When SiC particles were doped into the MREs, the internal CI aggregate structures were altered and formed stronger particle chains. Therefore, a large resistance will be yielded when a strain stimulus was applied. The SiC particles could bond well with polymer matrix and these particles would collaborate with the restrained polymer around particle chains to form much stronger aggregate structures. Thus, the SiC-strengthened MREs showed higher storage modulus than the nondoped one. When larger SiC particles were doped, the bonding will be weakened, and thus the corresponding aggregate structures could be damaged much easier. To this end, with increasing of the SiC sizes from 0.06 to 0.6 and 6 μm, a decrement of the storage modulus was found. In addition, SiC particles help to lock the aggregated structures in the polymer matrix, and this reinforce the strength of aggregated structures when SiC particles are small. With increasing of the average diameter of SiC, the locking effect will hinder the formation of the magnetic chains and finally the obstructions even outweigh the enhancement effect in sample MRE-6-SiC. Therefore, under applying the magnetic field, the storage modulus of the MRE-6-SiC was smaller than the nondoped MRE. If the size of the SiC particles was further increased to 60 μm, the SiC particles were too large to be integrated into the CI chains. In this case, the SiC particles play a reinforced effect on the polymer matrix, and thus the magnetic-dependent modulus increased.

Owing to the increment of the G_0, the relative MR effects of the SiC-strengthened MREs were inevitably decreased. The MR effect of the MRE-0.06-SiC was calculated to be 38.9% and the value was smaller than the nondoped MRE (40.6%). The G_0 of the MRE-0.06-SiC is about 2.16 times larger than the nondoped MRE, whereas the MR effect of the nondoped MRE is only 1.04 times larger than the MRE-0.06-SiC. In considering that fact, the actual weight ratio of the CI was decreased after introducing the SiC particles into the MRE, the low decrement of the MR effect may be responsible for the strengthening effect. The relative MR effects were influenced by size of the SiC particles and the values for the MRE-0.6-SiC, MRE-6-SiC, and MRE-60-SiC were 20.3, 29.9, and 38.2%, respectively.

The viscoelastic properties of the SiC-strengthened MREs were also highly influenced by the content of the SiC particles. As the better reinforcing behavior, 0.06-μm SiC particles were chosen to optimize the enhancement effect. By keeping other components as constant, the weights of the SiC particles were varied from 0 to 1.6, 3.2, and 4.8 wt%. Figure 2 shows that the magnetic field is dependent on the shear storage modulus for the SiC-strengthened MREs with different SiC contents. In comparison to the nonstrengthened MREs, the ΔG of the MRE strengthened with 1.6 wt% SiC particles increased from 0.12 to 0.15 MPa. With further increasing the weight fraction of SiC particles to 3.2 wt%, the ΔG increased to 0.25 MPa. However, too much of SiC particles were detrimental to the strengthening effect and the ΔG decreased to 0.11 MPa when the SiC particles further increased to 4.8 wt%. Excitingly, the MR effects of the MREs strengthened by the SiC particles also increased though the initial G_0 increased. If the SiC particles' con-

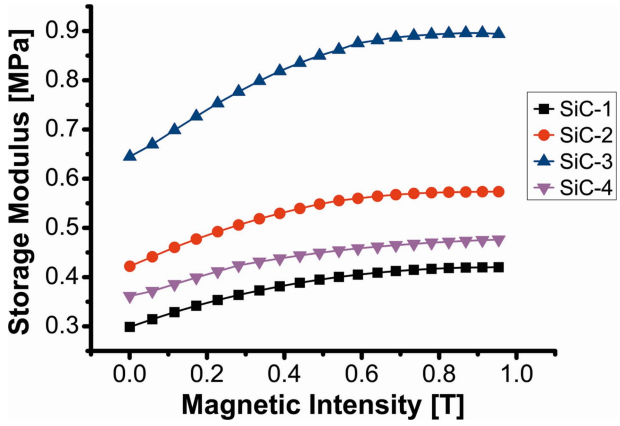

FIG. 2. The storage modulus of MRE samples with different SiC contents and the samples are tested at the stain amplitude of 0.2%. [Color figure can be viewed in the online issue, which is available at wileyonlinelibrary.com.]

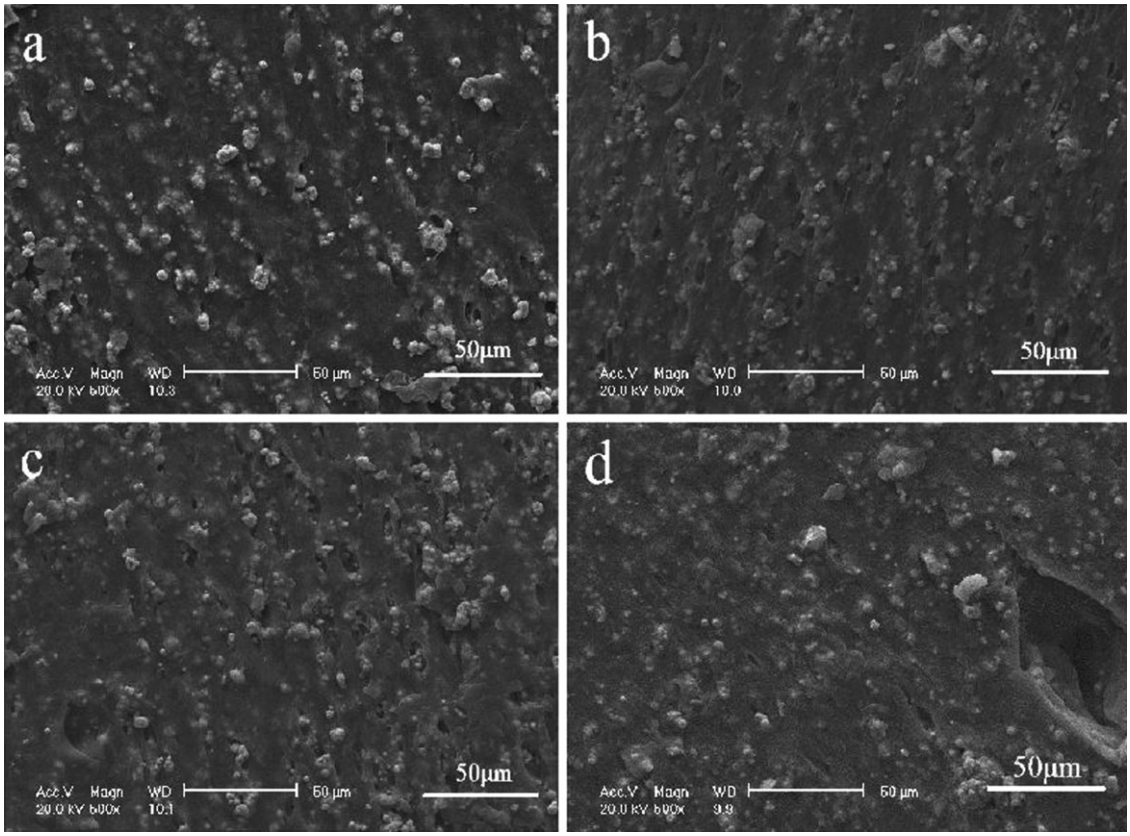

FIG. 3. The SEM images of the four samples: (a) MRE-0.06-SiC, (b) MRE-0.6-SiC, (c) MRE-6-SiC, and (d) MRE-60-SiC.

tent was 1.6 or 3.2 wt%, the MR effect was about 1.25 or 2.07 times larger than the traditional MREs without strengthening by the SiC particles, whereas the MR effect can keep only 94.6% for the MREs strengthened with 4.8 wt% SiC particles.

Based on the above analysis, the SiC-strengthened MREs with high viscoelastic properties can be obtained by optimizing the content and size of the SiC particles. Both the ΔG and the MR effect were improved by adding proper content of SiC particles with defined size. The incorporation of the SiC particles can enhance the viscoelastic performance of the MREs; however, too much of SiC additives are harmful for the enhancement of the relative MR effect and the optimum SiC content was estimated to be 3.2 wt% of 0.06 μm SiC particles.

To better understand the influence of the SiC particles on the mechanical property of the MREs, the internal structures of the SiC-strengthened MREs were investigated. Figure 3 shows the SEM images of the MREs strengthened by SiC particles with different sizes. In these samples, the content of the iron (60 wt%) and SiC particles (3.2 wt%) was kept under the same value, whereas the diameters of the SiC particles were varied from 0.06 to 0.6, 6, and 60 μm, respectively. All the products exhibited typical chain-like structures and the particles were well bonded to the rubber matrix. It was observed that the particle chains shown in Fig. 3a and d were more obvious and stouter than the other two samples (Fig. 3b and c). In comparison to the MRE-0.06-SiC, the particle chains for the MRE-0.6-SiC were slimmed and shorted. With increasing of the size to 6 μm (Fig. 3c), the chains become unclear which may be owing to the disturbance of the SiC particles. The SiC and the iron particles cannot be distinguished by using the SEM testing, and thus the chain structure was indistinct for MRE-0.6-SiC and MRE-6-SiC as the size of the SiC particles was similar to the iron particles. When the SiC size was further increased to 60 μm, the disturbance of the SiC decreased, the particle chains become stout and strong again and they were more obvious than those in sample MRE-0.6-SiC and MRE-6-SiC. Therefore, the diameter of SiC shows different effects on altering the microstructures of MREs.

Figure 4 shows the SEM images of SiC-strengthened MRE with different contents of 0.06 μm SiC particles (0, 1.6, 3.2, and 4.8 wt%). For the nonstrengthened sample (Fig. 4a), the CI particles assembled along the magnetic field and chain-like microstructure can be clearly observed. After doping 1.6 wt% SiC particles into the MRE, the chain structure was well kept, which indicated the presence of the SiC particles did not break this kind of orderable structures. With increasing of the SiC content

 DOI 10.1002/pen

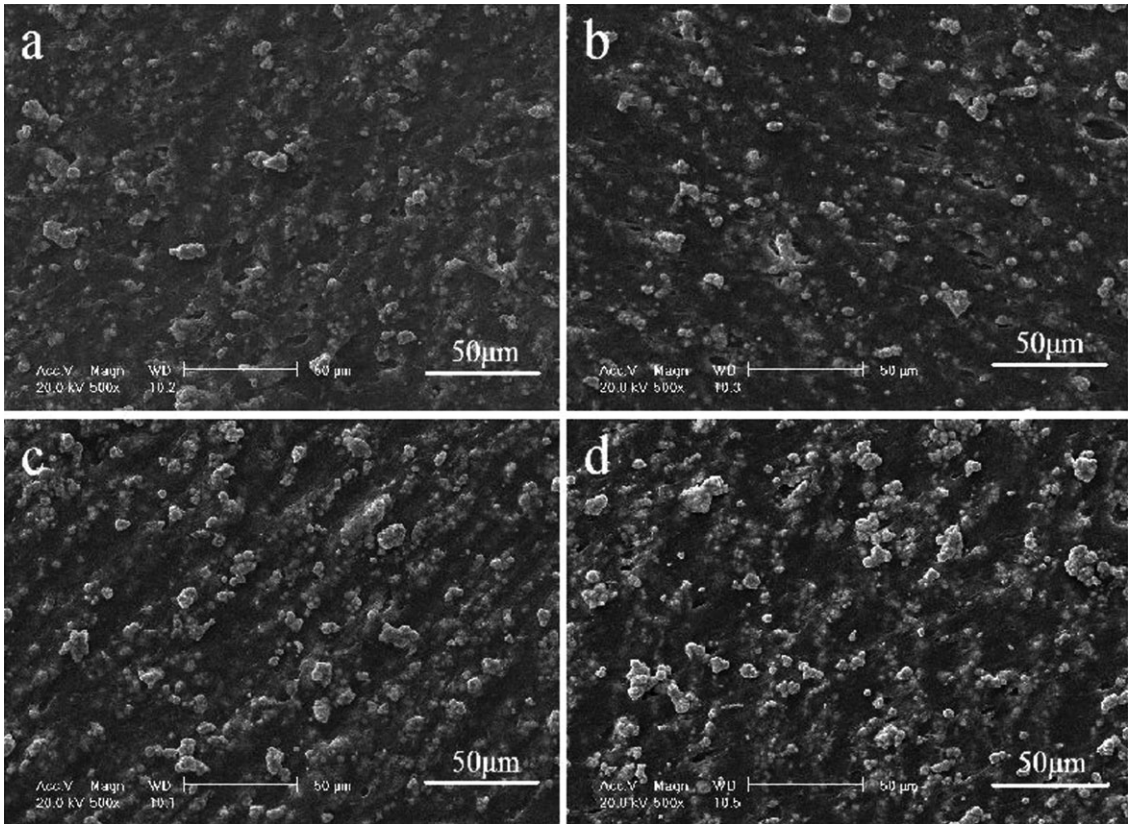

FIG. 4. The microstructure of the four samples: (a) MRE-0.06-SiC-1, (b) MRE-0.06-SiC-2, (c) MRE-0.06-SiC-3, and (d) MRE-0.06-SiC-4.

to 3.2 wt%, the particle chains became more obvious and stouter (Fig. 4c). However, when the SiC weight content further increased to 4.8 wt%, the particle chains were disturbed. As shown in Fig. 4d, the particle chains in MREs were shorter and less regular than those shown in Fig. 4a–c. Therefore, the microstructures of CI particle chains were altered by doping the SiC particles. When the weight content of SiC particles reached 3.2 wt%, the microstructures of CI particle chains were most regular and obvious. However, further increasing of the weight content of the SiC particles will hinder the chain's formation. With increasing of the SiC content, the G_0 of MREs increases, which means the increment of the stiffness. Here, the increment of the ΔG may be responded to the transformation of the microstructures. From the SEM image (Fig. 4), we can find that the internal aggregated structures of the iron particles changed accordingly when the SiC particles were doped into the MREs. If the SiC content was smaller than 3.2 wt%, the internal aggregate structures were strengthened. The as-prepared composites will yield greater resistance to the external strain under applying an external magnetic field, thus the ΔG of the MREs increases. However, when the SiC content exceeds 3.2 wt%, the internal friction of SiC particles will hinder the formation of aggregate structures. As a result, a decrease of the ΔG was found in the MRE-0.06-SiC-4.

The Influence of the SiC Particles on the Damping Properties of the SiC-Strengthened MREs

Damping was a crucial parameter that evaluates a material's energy dissipation capacity. Usually, the damping capacity was evaluated by loss tangent (tan ϕ), loss factor (η), specific damping capacity (ψ), logarithmic decrement (δ), and inverse quality factor (Q^{-1}) [33]. The relationship between these factors was as follows:

$$\phi = \tan\phi = \eta = Q^{-1} = \delta/\pi = \psi/2\pi \tag{1}$$

In this study, we use the loss tangent (tan ϕ) to evaluate the damping capacity of MRE samples.

The influence of the SiC particles on the damping property of the MREs was studied to analyze the enhancing effect. Figure 5 shows the loss modulus of the SiC-strengthened MREs, which were tested under the strain amplitude of 0.2%. Under applying a magnetic field, the loss modulus first increased and then turned to be level off as soon as the magnetic particles were magnetically saturated. In comparison to the traditional MREs, the SiC-strengthened MREs exhibited higher loss modulus when the 0.06 μm SiC particles were used. The initial loss modulus is 0.164 MPa in 0.06 μm SiC-strengthened MRE, which is larger than the nondoped one (0.071 MPa). When the size of SiC increased to 0.6 and 6 μm,

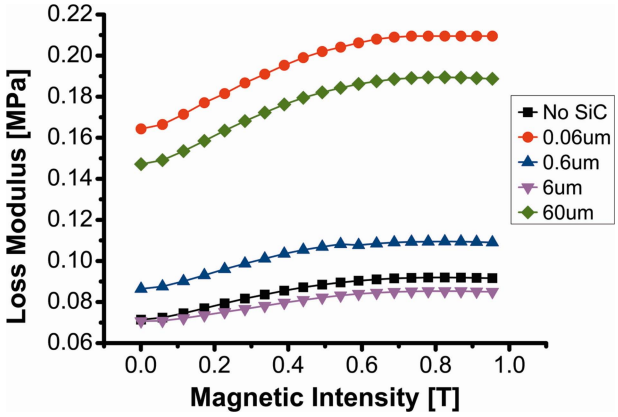

FIG. 5. The loss modulus of MRE samples strengthened with different SiC sizes and tested at strain amplitude of 0.2%. [Color figure can be viewed in the online issue, which is available at wileyonlinelibrary.com.]

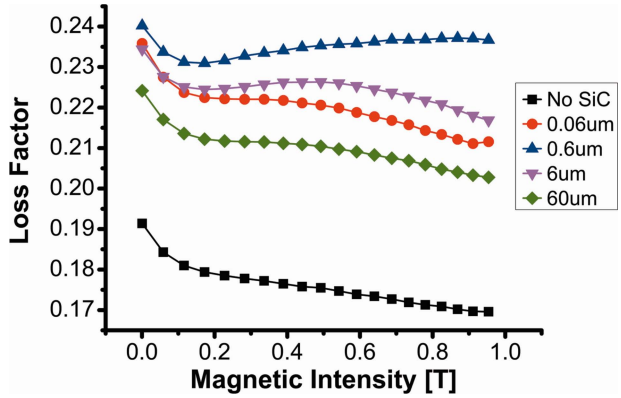

FIG. 7. The damping factor of different diametric SiC-doped MRE samples and the samples are tested at the strain amplitude of 0.2%. [Color figure can be viewed in the online issue, which is available at wileyonlinelibrary.com.]

the loss modulus of the SiC-strengthened MREs decreased to 0.086 and 0.070 MPa. However, the loss modulus sharply increased when the diameter of SiC particles further increased to 60 μm. Clearly, this phenomenon was very similar to the magnetic-dependent storage modulus, which may also be responded for the change of the ordered microstructures.

The loss modulus increased with the SiC content and reached the highest value when the SiC content reached 3.2 wt%. However, when the SiC content increased to 4.8 wt%, the loss modulus sharply decreased. As shown in Fig. 6, the initial loss modulus of the SiC-strengthened MREs increased from 0.071 MPa (MRE-0.06-SiC-1) to 0.164 MPa (MRE-0.06-SiC-3). However, with further increasing of the SiC content to 4.8 wt%, the initial loss modulus decreased to 0.050 MPa. Generally, the loss modulus of SiC-strengthened MREs exhibited an enhanced nature till the content of SiC particles reached a critical value.

As soon as the SiC particles were doped into the MREs, the damping factor sharply increased in comparison to the nonstrengthened MRE. Figure 7 shows the damping factor of the MREs strengthened with different sized SiC particles, in which the damping factor decreased with increasing of the magnetic field. Unfortunately, the dependence of the SiC particles size on the damping factor was irregular. With the SiC particles' size increased from 0.06 to 0.6 μm, the damping factor increased. However, the further increasing of the SiC particles size to 6 and 60 μm lead to the decrement of the damping factor. The MRE was a kind of special particle-reinforced materials. After introducing SiC particles, the friction between the particles and the interaction force between the particles and the polymer matrix increased, and thus the damping factor of the SiC-strengthened MREs increased. As the microstructures of the SiC-strengthened MREs varied with different kinds of SiC particles, the damping property was highly influenced by the SiC particle sizes. Similarly, an optimum SiC particle content was also found to achieve the best damping property. Figure 8 shows the damping factor of SiC-strengthened MREs with different SiC contents (0.06 μm). The damping factor increased with increasing of the SiC content. As soon as the content increased to 3.2 wt%, the damping factor decreased.

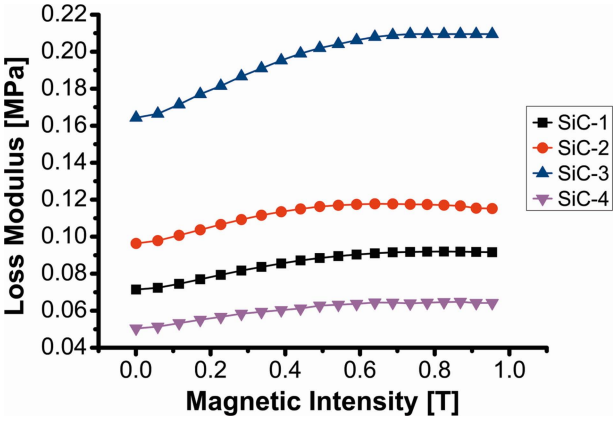

FIG. 6. The loss modulus of MRE samples with different SiC contents and the samples are tested at strain amplitude of 0.2%. [Color figure can be viewed in the online issue, which is available at wileyonlinelibrary.com.]

The Influencing Mechanism of the SiC Particles on the Viscoelastic Properties of the SiC-Strengthened MREs

Based on the above analysis, the storage modulus of MREs was classified into two parts: one is the intrinsic storage modulus of each component and the other is the magneto-induced storage modulus of the magnetic particles. For the intrinsic storage modulus, the particles are treated as ellipsoid inclusions in the matrix and they can enhance the overall storage modulus. By the Eshelby inclusion theory, the overall storage modulus could be written as [22, 34]

$$G_C = V_m G_m + V_p G_p + V_n G_n \quad (2)$$

where G_C denotes the initial shear modulus of MREs, G_m denotes the shear modulus of matrix material, G_p is the

DOI 10.1002/pen

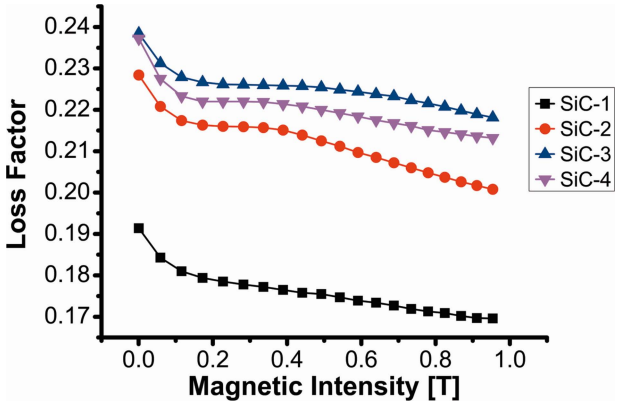

FIG. 8. The damping factor of MRE samples doped with different contents of 0.06 μm SiC and the samples are tested at the strain amplitude of 0.2%. [Color figure can be viewed in the online issue, which is available at wileyonlinelibrary.com.]

shear modulus of CI particle, G_n is the shear modulus of the SiC particle, V_m is the volume fraction of matrix, V_p is the volume fraction of CI particle, V_n is the volume fraction of SiC particles.

Shen et al. [35] had proposed a mathematical model to estimate the magneto-induced storage modulus by considering all the dipole interactions in a chain and the nonlinear properties of the host composite, which agreed with the experimental data. Based on their study, the magneto-induced storage could be written as [35]

$$\Delta G = 9\frac{\phi C m^2(4-\tau^2)}{r_0^2\pi^2 d^3\mu_0\mu_1(1+\tau^2)^{7/2}} \tag{3}$$

where ϕ is the volume fraction of CI particles in MREs and $\phi = V_p/(V_m + V_p + V_p)$, d is the diameter of the CI particle, μ_0 denotes the vacuum permeability, $\mu_0 = 4\pi \times 10^{-7}$ H m^1, μ_1 is the permeability of MREs, r_0 is the initial spacing between the two adjacent dipoles, $\tau$is the shear strain, and m is the magnetic dipole moment. For simplicity, m is assumed to be the same in each particle in a single chain.

Therefore, the overall storage modulus of the SiC-strengthened MREs could be written as

$$G_{MRE} = V_m G_m + V_p G_p + V_n G_n + 9\frac{\phi C m^2(4-\tau^2)}{r_0^2\pi^2 d^3\mu_0\mu_1(1+\tau^2)^{7/2}} \tag{4}$$

Therefore, from *Eq. 4*, it could be observed that the parameters that determine the overall storage modulus are the volume fraction of each component, the strain amplitude, and the mean diameter of CI particles. If the size of the SiC particles, matrix content, and CI content was kept constant, the storage modulus increased with increasing of the SiC content under applying the same strain amplitude. Owing to the incorporation of SiC particles, the initial central distance between two adjacent magnetic CI particles r_0 was shortened, which can be seen in microstructures change (Fig. 3). Therefore, the storage modulus of MRE was changed with the SiC size and content.

From *Eq. 4*, it can be found that storage modulus decreases with increasing of the strain amplitude, which agreed well with the previously published literatures [36]. Moreover, the viscoelastic property of the SiC-strengthened MREs was dependent on the SiC size and can also be explained by these equations. The SiC particles can enhance the strength of magnetic particle chains. When the size of the SiC particles increases, the bonding between the particles and the matrix material is weakened, and thus the contribution of intrinsic shear modulus of SiC particles decreases. Therefore, the storage modulus changes with the size of the SiC particles (Fig. 1).

The damping capacity of MREs can be approached by referring to the method used in traditional particle-reinforced particles. As the CI particles are soft magnetic particles, the magnetic damping is minimal and thus it is ignored in this study. Consequently, the damping of the MRE was expressed in the following equation [36]:

$$D_{MRE} = D_C + D_I \tag{5}$$

where D_C is the intrinsic damping of each component, D_I is the interface damping between the reinforced particles and the rubber matrix.

It is worth noting that the intrinsic damping of reinforced particles, including the CI particles and the SiC particles, is negligible compared with the intrinsic damping of rubber matrix. Then, the intrinsic damping of MRE is simplified as

$$D_C = (1-\phi)D_m \tag{6}$$

where ϕ is the volume fraction of CI particle, D_m represents the damping property of matrix material.

The interfacial damping is mainly caused by internal friction [37]. Figure 9 shows the scheme of internal fic-

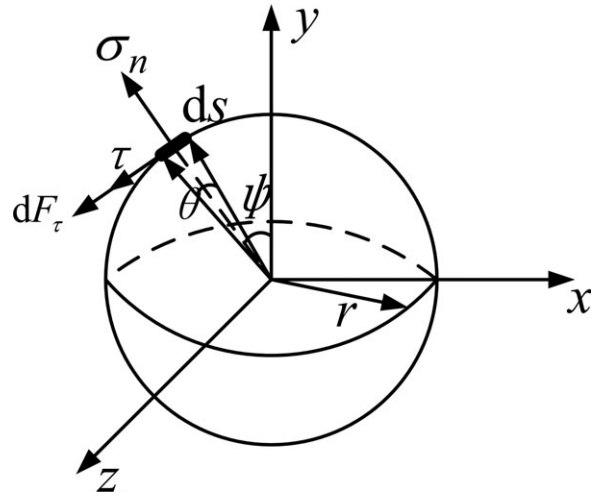

FIG. 9. The schematic diagram of interface damping.

tion at the interfaces between the reinforced particles and the matrix material, and ds denote the area increment where the reinforcing particles and the matrix material have a relative motion trend, τ and σ are the tangential and normal stress at ds, dF_τ is the fiction increment at ds. Assuming the interfacial condition between reinforced particles and matrix materials is either strong or weak, and thus the interface damping of MREs is expressed as

$$D_{\mathrm{I}} = \varphi \frac{117}{76\pi^2}\phi + (1-\varphi)K\frac{3\pi}{2}\frac{f\sigma_r}{\sigma_0}V\phi \tag{7}$$

where φ denotes the proportion of strongly interfacial bonds, f is the frictional coefficient between the CI particles and the rubber matrix, σ_0 is the stress loaded upon the MRE sample, σ_{r} is the corresponding stress at the surface where the CI particles have a relative motion to the rubber matrix.

Therefore, the nonmagnetic damping of MREs is obtained as

$$D_{\mathrm{MRE}} = (1-\phi)D_{\mathrm{m}} + \phi D_{\mathrm{p}} + \varphi\frac{117}{76\pi^2}\phi + (1-\varphi)K\frac{3\pi}{2}\frac{f\sigma_r}{\sigma_0}V\phi \tag{8}$$

As derived in *Eq. 8*, it is clear that the two main factors collaborate to determine the total damping capacity: the content of magnetic particles (ϕ), the condition of the interfaces (φ). Large interfaces also lead to the increment in the interface damping.

Therefore, the size-dependent damping capacity of the SiC-strengthened MRE was mainly determined by the different interface dampings. The difference for the SiC particles' sizes leaded to the different interface damping. As the sizes of SiC particles increased, the interfacial bondage between the SiC particles and the matrix materials changed accordingly. For the sample MRE-0.06-SiC, most of the interfacial bondages were well bonded, whereas most of the interfaces are weakly bonded for the sample MRE-60-SiC. As indicated in *Eq. 8*, the interface damping is the summation of strongly bonded interfaces damping and weakly bonded interfaces. In the four samples, with increasing of SiC particles' sizes, the damping contributed by strongly interfacial damping decreased and the contribution owing to the weakly bonded interfaces increased. Therefore, the damping of MRE-0.06-SiC was smaller than the other ones of MRE-0.6-SiC and MRE-6-SiC. However, it was worth noting that stress concentration coefficient $\sigma_{\mathrm{r}}/\sigma_0$ decreased with the diameter of the reinforced particles. Therefore, as the diameter of SiC particles increased, the damping contributed by weakly bonded interfaces was less significant than doping with smaller diametric SiC particles. Consequently, the damping factor in MRE-6-SiC and MRE-60-SiC was lower than the one in MRE-0.06-SiC. Furthermore, with increasing of the SiC content, the damping factor of the SiC-strengthened MRE increased. However, when the SiC content exceeded the critical value 3.2 wt%, the SiC particles tended to be agglomerated and thus hindered the formation of particle chain, and then the damping factor decreased. Simultaneously, the condition of the interfaces was affected by the strain amplitude, and thus the increasing strain amplitude leads to an increasing interface damping capacity, which agreed well with the experimental results (Fig. 8).

CONCLUSIONS

In this study, novel kind of SiC-strengthened MREs was developed and their viscoelastic properties were studied. In comparison to the traditional MREs, the SiC-strengthened MREs exhibited higher G_0, ΔG, and damping property when the content of SiC particles increased to an optimum value (3.2 wt%). Besides the content, the size of the SiC particles was also proven to be a critical role to dominate the viscoelastic property of the samples. Based on the analysis, the enhancement mechanism of the SiC particles on the viscoelastic properties was systematically investigated. Under the same condition, the storage modulus increment in MRE-0.06-SiC-3 was almost 2.08 times of MRE-0.06-SiC-1, and MR effect remained unchanged. As a result, this study supplied a useful method to control the viscoelastic property of the MREs, which may be applied in damper, vibration control, isolator, and so on.

REFERENCES

1. G. Filipcsei, I. Csetneki, A. Szilagyi, and M. Zrinyi, *Adv. Polym. Sci*., **206**, 137 (2007).
2. D.V. Juan, D.J. Klingenberg, and H.A. Roque, *Soft Matter*., **7**, 3701 (2011).
3. C. Ruddy, E. Ahearne, and G. Byrne, *Proc. SPIE,* **3675**, 131 (1999).
4. M.R. Jolly, J.D. Carlson, B.C. Munoz, and T.A. Bullions, *J. Intell. Mater. Syst. Struct*., **7**, 613 (1996).
5. J.M. Ginder, M.E. Nichols, L.D. Elie, and J.L. Tardiff, *Smart Struct. Mater*., **3675**, 131 (1999).
6. M. Farshad and A. Benine, *Polym. Test*., **23**, 347 (2004).
7. M. Kallio, T. Lindroos, and S. Aalto, "The Elastic and Damping Properties of Magnetorheological Elastomers," in *Internal Symposium on Applied Materials*. Espoo, FINLAND Technical Research Centre of Finland (2006).
8. X.Z. Zhang, W.H. Li, and Y. Zhou, "A Variable Stiffness Mr Damper for Vibration Suppression," in *2009 IEEE/ASME International Conference on Advanced Intelligent Mechatronics*. Singapore: 2009 IEEE/ASME International Conference on Advanced Intelligent Mechatronics (AIM) (2009).
9. H. Boese, A. Hesler, G. Monkman, and H. Bose, Magnetorheological Material Made of Non-Magnetizable Elastomers and/or Thermoplastic Elastic Carrier Medium, Useful E.G.

As Actuators and Safety Switches, Comprises a First Sort of Magnetizable Particle Made from a Hard Magnetic Material, Fraunhofer Ges Foerderung Angewandten Ev (2009).
10. D. York, X.J. Wang, and F. Gordaninejad, *J. Vibration Acoust. Trans. ASME*, **133**, 031003 (2011).
11. Z.G. Ying, H.F. Chen, and Y.Q. Ni, "Magneto-Rheological Visco-Elastomer and Its Application to Suppressing Micro-Vibration of Sandwich Plates," in *Third International Conference on Smart Materials and Nanotechnology in Engineering*. Shenzhen, PEOPLES R CHINA Proceedings of SPIE (2012).
12. A. Boczkowska and S.F. Awietjan, "Tuning Active Magnetorheological Elastomers for Damping Applications," in *5th International Materials Symposium/14th Conference of the Sociedade-Portuguesa-de-Materiais*. Lisbon, PORTUGAL ADVANCED MATERIALS FORUM V (2010).
13. K.M. Popp, X.Z. Zhang, W.H. Li, and P.B. Kosasih, *J. Intell. Mater. Syst. Struct.*, **21**, 1471 (2010).
14. B.J. Park, F.F. Fang, and H.J. Choi, *Soft. Matter.*, **6**, 5246 (2010).
15. J.K. Wu, X.L. Gong, Y.C. Fan, and H.S. Xia, *J. Appl. Polym. Sci.*, **123**, 2476 (2012).
16. B. Nayak, S.K. Dwivedy, and K.S.R.K. Murthy, *Int. J. Nonlinear Mech.*, **47**, 448 (2012).
17. J.L. Mietta, M.M. Ruiz, P.S. Antonel, O.E. Perez, A. Butera, G. Jorge, and R. Martin Negri, *Langmuir*, **28**, 6985 (2012).
18. X.S. Lu, X.X. Qiao, H. Watanabe, X.L. Gong, T. Yang, W. Li, K. Sun, M. Li, K. Yang, H.G. Xie, Q. Yin, D. Wang, and X.D. Chen, *Rheol. Acta*, **51**, 37 (2012).
19. S.A. Demchuk and V.A. Kuz'min, *J. Eng. Phys. Thermophys.*, **75**, 103 (2002).
20. M. Lokander and B. Stenberg, *Polym. Test.*, **22**, 677 (2003).
21. J.F. Li, X.L. Gong, Z.B. Xu, and W.Q. Jiang, *Int. J. Mater. Res.*, **99**, 1358 (2008).
22. W.H. Li and X.Z. Zhang, *Smart Mater. Struct.*, **19**, 035002 (2010).
23. W. Zhang, X.L. Gong, S.H. Xuan, and Y.G. Xu, *Ind. Eng. Chem. Res.*, **49**, 12471 (2010).
24. W.Q. Jiang, Y.L. Zhang, S.H. Xuan, C.Y. Guo, and X.L. Gong, *J. Magn. Magn. Mater.*, **323**, 3246 (2011).
25. L. Chen, X.L. Gong, and W.H. Li, *Polym. Test.*, **27**, 340 (2008).
26. J.M. Ginder, M.E. Nichols, L.D. Elie, and J.L. Tardiff, "Magnetorheological Elastomers: Properties and Applications," in *The SPIE Conference on Smart Materials Technologies*, Newport Beach, California. SPIE, **3675**, 131 (1999).
27. H.N An, S.J. Picken, and E. Mendes, *Soft Matter.*, **6**, 4497 (2010).
28. J.K. Wu, X.L. Gong, L. Chen, H.S. Xia, and Z.G. Hu, *J. Appl. Polym. Sci.*, **114**, 901 (2009).
29. Y.C. Fan, X.L. Gong, W.Q. Jiang, W. Zhang, B. Wei, and W.H. Li, *Smart Mater. Struct.*, **19**, 055015 (2010).
30. P. Colomban, *Adv. Eng. Mater.*, **4**, 535 (2002).
31. L.V. Interrante, K. Moraes, W. Sherwood, J. Jacobs, and C. Whitmarsh, "Low Cost, near Net Shape Ceramic Composites by Polymer Infiltration and Pyrolysis," in *Proceedings of the Eighth Japan-U.S. Conference on Composite Materials*, Baltimore, MD (1999).
32. S.Y. Shao, P. Yang, G. Wang, and J. Zhang, *Chem. Ind. Times*, **24**, 25 (2010).
33. E.J. Lavernia, R.J. Perez, and J. Zhang, *Metall. Mater. Trans. A*, **26A**, 2803 (1995).
34. L.C. Davis, *J. Appl. Phys.*, **85**, 3348 (1999).
35. Y. Shen, M.F. Golnaraghi, and G.R. Heppler, *J. Intell. Mater. Syst. Struct.*, **15**, 27 (2004).
36. L. Chen, X.L. Gong, and W.H. Li, *Chin. J. Chem. Phys.*, **21**, 581 (2008).
37. E.J. Lavernia, J. Zhang, and R.J. Perez, *Key Eng. Mater.*, **104–107**, 691 (1995).